THE JOURNAL OF PHYSICAL CHEMISTRY Letters

Letter

pubs.acs.org/JPCL

Enhanced Organo-Metal Halide Perovskite Photoluminescence from Nanosized Defect-Free Crystallites and Emitting Sites

Yuxi Tian,[†] Aboma Merdasa,[†] Eva Unger,[†] Mohamed Abdellah,[†] Kaibo Zheng,[†] Sarah McKibbin,[‡] Anders Mikkelsen,[‡] Tõnu Pullerits,[†] Arkady Yartsev,[†] Villy Sundström,[†] and Ivan G. Scheblykin*[,†]

[†]Chemical Physics, Lund University, Box 124, SE-22100 Lund, Sweden

[‡]Division of Synchrotron Radiation Research, Lund University, Box 118, 221 00 Lund, Sweden

Supporting Information

ABSTRACT: Photoluminescence (PL) of organo-metal halide perovskite semiconductors can be enhanced by several orders of magnitude by exposure to visible light. We applied PL microscopy and super-resolution optical imaging to investigate this phenomenon with spatial resolution better than 10 nm using films of $CH_3NH_3PbI_3$ prepared by the equimolar solution-deposition method, resulting in crystals of different sizes. We found that PL of ∼100 nm crystals enhances much faster than that of larger, micrometer-sized ones. This crystal-size dependence of the photochemical light passivation of charge traps responsible for PL quenching allowed us to conclude that traps are present in the entire crystal volume rather than at the surface only. Because of this effect, "dark" micrometer-sized perovskite crystals can be converted into highly luminescent smaller ones just by mechanical grinding. Super-resolution optical imaging shows spatial inhomogeneity of the PL intensity within perovskite crystals and the existence of <100 nm-sized localized emitting sites. The possible origin of these sites is discussed.

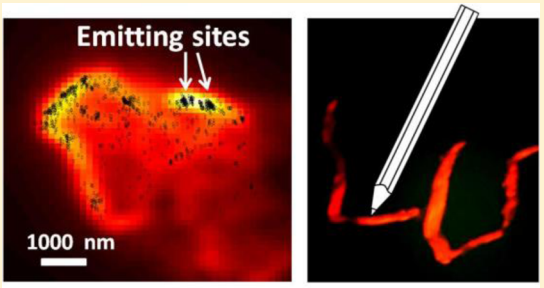

Organo-metal halide (OMH) perovskites have attracted much attention in last several years as they are very promising materials for solar energy conversion, electroluminescence, and even lasing.[1,2] Bright photoluminescence (PL),[3,4] the possibility to tune the emission wavelength,[5] and preparation of nanoparticles[6−8] as well as PL blinking effect[9−11] makes OMH perovskites interesting also for fluorescence imaging applications.

Many of the fundamental electronic and optical properties of these hybrid semiconductor materials are still far from being understood.[1,2,12] The PL has been reported to be strongly dependent on many factors such as excitation power density, chemical treatment, environment and the sample preparation method.[2,4,8,13,14] How the sample is prepared controls the nano- and microstructure of the sample as well as the nature, location (bulk vs surface), and concentration of defects.[15−18] Furthermore, the PL varies and fluctuates in the course of light irradiation during a measurement, making the investigation more challenging.[9,14,19]

Photoluminescence microscopy combined with spectroscopy allows us to study the photoluminescence dynamics of a sample with high spatial resolution. This method is therefore a powerful tool in the characterization of polycrystalline semiconductor materials because local variations in photophysical properties can be investigated. Such studies have shown a dependence of the OMH perovskite electronic properties on crystal size, shape, and spatial location inside the perovskite crystals.[9,10,20−25] Variations in trap state density in different domains of a polycrystalline sample can be visualized by a PL microscopy image.[9,21,23] By combining this method with other experimental techniques such as scanning electron microscopy (SEM) and X-ray spectroscopy, local differences in PL dynamics can be correlated with the inhomogeneity in the material composition and morphology.[21]

The particular phenomenon we will elaborate on in this contribution is the light-induced PL enhancement observed in perovskite films prepared by solution-deposition methods.[9,14,19] The phenomenon manifests as an increase in PL by several orders of magnitude during light exposure of the sample. Because light illumination does not change the optical density of the films, this implies that the PL quantum yield of the as-prepared samples was initially very low ($<10^{-3}$). Low PL quantum yield of the as-prepared perovskite samples suggests that there are defects that act as PL quenchers. PL quenching has been assigned to charge-carrier trapping on intraband trap states causing nonradiative Shockley−Reid−Hall recombination.[1,15,19,25−29] As we will show, light-irradiation under ambient conditions removes, or deactivates, the traps leading to the observed increase in PL. Recent studies of the PL enhancement effect in different atmospheres[11,13] and our own experiments[30] showed that this occurs through a photochemical reaction involving oxygen. We report the crystal size dependence of this effect, which indicates that these quenching sites are situated throughout the crystals, rather than on the surface

Received: September 14, 2015
Accepted: October 1, 2015
Published: October 1, 2015

DOI: 10.1021/acs.jpclett.5b02033
J. Phys. Chem. Lett. 2015, 6, 4171−4177

of the crystals only. For the first time we applied a super-resolution optical imaging technique to several micrometer-sized perovskite objects. It appeared that the intensive PL reached by trap-deactivation is often coming from localized areas inside perovskite conglomerates, which we call emitting sites. A possible nature of the emitting sites will be discussed.

We start our report by presenting an interesting new observation that the enhancement of PL quantum yield of a perovskite film can be triggered by mechanical grinding of the perovskite crystals under ambient conditions. Figure 1a shows a

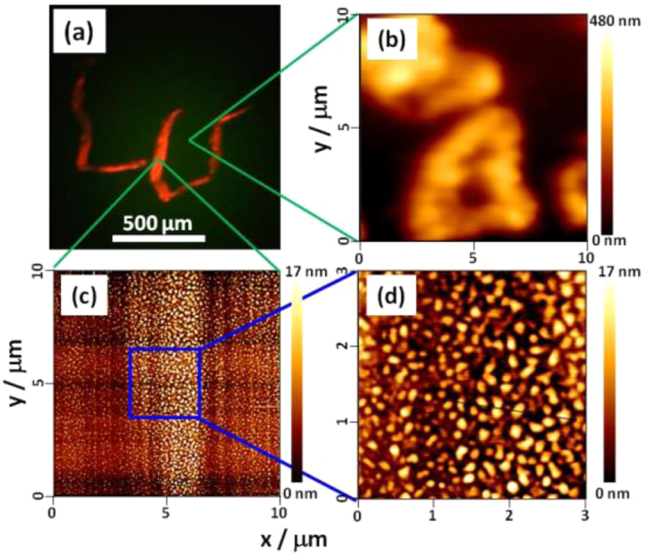

Figure 1. Enhanced PL of a mechanically scratched $CH_3NH_3PbI_3$ perovskite film prepared on glass. (a) "LU" was written on the film by a metal needle. The image was taken by Nikon D500 color camera via a fluorescence microscope using 2× objective lens; excitation power was ~0.5 W/cm^2. Comparison of AFM images of the as-prepared area of the film (b) and the scratched area (c). (d) Zoom of panel c shows that the needle ground the micrometer-sized perovskite crystals to particles <100 nm in size.

luminescence image where the letters "LU" were scratched into the $CH_3NH_3PbI_3$ perovskite film using a metal needle and appear as a bright image with respect to the background. (See the video of the "writing process" in the Supporting Information (SI), Movie 1.) In this image the PL intensity (per unit area) from the scratches is more than 1 order of magnitude higher than that from the rest of the film.

We compared the morphology of the crystals within and outside the scratched area. The AFM images in Figure 1 show that mechanical scratching of the perovskite film ground several micrometer large crystals (Figure 1b) to smaller crystals with sizes <100 nm (Figure 1c and 1d). The PL spectrum of the scratched part is ~10 nm blue-shifted compares with the spectrum of large crystals (Figure 2 inset). This spectrum is identical to the PL spectra of $CH_3NH_3PbI_3$ nanocrystals previously reported (shown by a thin black line in Figure 2 inset).[9] We assign this small shift of the PL spectra to self-absorption in the larger crystals. Hence, we conclude that the mechanical treatment forms smaller crystals, and this leads to an increased PL quantum yield of the perovskite material under our experimental conditions.

We took a closer look at the time dependence of the PL intensity of the scratched and as-prepared regions of the sample under the same light irradiation conditions. Figure 2 shows that

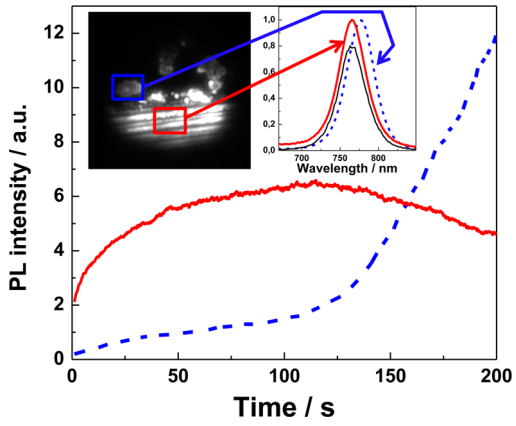

Figure 2. Light-induced PL enhancement of scratched part (red line) and untreated part (blue dashed lines) of the same $CH_3NH_3PbI_3$ film. The PL image in the inset shows the areas of the film where the PL intensity traces and PL spectra were collected. The excitation power density was similar for these two areas (1 W/cm^2). The inset also shows (thin black line) the PL spectrum for blinking $CH_3NH_3PbI_3$ nanocrystals reported in ref 9 for comparison (scaled for clarity). The spectrum of the scratched areas of the film and the nanocrystals is identical.

the PL of the scratched region was increasing at a much faster rate compared with the as-prepared region. Moreover, the initial PL intensity (per unit area) of a scratched region was about 1 order of magnitude larger than that of the as-prepared region. That is why the mechanical scribe appeared bright red on a dark background in Figure 1a. Within the time-resolution of our experiment (100 ms) we were not able to determine whether the PL quantum yield was high from the very beginning or it was enhanced within 100 ms due to the light treatment. (See Movie 1 that shows the real time writing on the film in the SI.) Prolonged irradiation leads to a further increase in PL on the time scale of tens of seconds, followed by clear degradation. The observed effect of the crystal grinding suggests that the PL enhancement dynamics is dependent on the crystal size.

To further substantiate the crystal size-dependence of the PL enhancement, we measured PL enhancement kinetics for individual crystals of different sizes that can be resolved by the optical microscope as shown in Figure 3a–c. Small crystals (lateral dimension <300 nm), observed as diffraction-limited spots in the microscope (Figure 3a), exhibit an almost instant (several seconds at most) increase and saturation of the PL accompanied by PL blinking. In comparison, middle-sized (Figure 3b) and large crystals (tens of micrometers, Figure 3c) exhibit a much slower increase in the PL under the same illumination conditions. AFM measurements showed that crystals with larger facial dimensions possessed also larger thickness (see, e.g., Figure 1b); this will become important for the discussion below. Thus, clear positive correlation between the PL enhancement characteristic time and the crystal size was observed (Figure 3d). Although the particular characteristic times varied from sample to sample, the same positive correlation between the crystal size and PL characteristic enhancement time was always observed for all studied samples.

How can we rationalize the crystal size dependence of the PL enhancement? Or, in other words, why is the speed of the photochemical reaction deactivating the trapping sites dependent on the crystal size? Reaction rates in heterogeneous systems depend on the interfacial area between the phases and mutual

DOI: 10.1021/acs.jpclett.5b02033
J. Phys. Chem. Lett. 2015, 6, 4171−4177

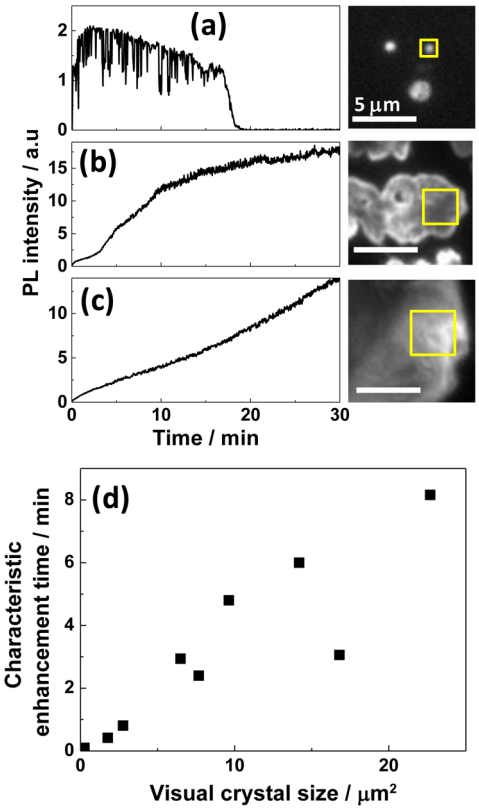

Figure 3. Crystal size dependence of the PL enhancement effect. PL intensity traces of $CH_3NH_3PbI_3$ perovskite crystallites of different sizes: (a) small, (b) middle, and (c) large. The right column shows the corresponding PL images and the selected region for analysis. (d) Correlation between the characteristic enhancement time (time to reach $(1 - 1/e) = 0.63$ of the saturation intensity) and the visual crystal size; all data points were measured from the same sample. The excitation power density was 0.5 W/cm^2.

penetration of the reacting components. The herein described case is a reaction involving the solid crystal, oxygen, and light-generated electrons. The 1/e penetration depth of the excitation light (λ = 514 nm) to the intact crystals is ∼100 nm, as calculated from the published Napierian absorption coefficient.[31,32] Because the light-generated electrons are necessary for the reaction, it is in an ∼100 nm thick layer that the trap deactivating reaction occurs initially. This is what happens for small nanocrystals where the trap deactivation reaction takes less than a few seconds and should also happen in the surface layer of thick crystals. The observation of much slower PL enhancement for large and thick crystals leads to the conclusion that (i) the traps are not only at the surface but must also be in the interior (bulk) of the crystals and (ii) the reaction rate in the depth of the crystal is slower than in the surface layer.

Let us consider the process in more detail. The reaction rate slows down toward the interior of the material because the light intensity, and thus concentration of charge carriers needed for the reaction, decreases exponentially with distance from the surface. As-prepared perovskite samples with a PL quantum yield as low as 10^{-3} exhibit trap-controlled PL lifetimes of just a few nanoseconds,[30] which leads to short (<100 nm) charge diffusion lengths.[32] Note that such short PL lifetime of solution-prepared $CH_3NH_3PbI_3$ samples is known in the literature[32,33] and that the impressive micrometer long diffusion length in OMH perovskite was reported for samples with PL lifetimes as long as several hundred nanoseconds and correspondingly high PL yield close to unity.[4,33] Thus, because the charge diffusion length is initially short the reaction zone must be indeed initially limited by the light penetration depth, which is ∼100 nm under our experimental conditions. After some light exposure when more and more traps become passivated in the layer close to the surface, the excited electrons can diffuse deeper inside the crystal, making the reaction zone spread further to the interior of the crystal, leading to the observed slow "curing" of the whole volume of a thick crystal. The "fuel" for the curing of the PL quenching traps is oxygen.[13,30] Because our samples were prepared under ambient conditions with oxygen-containing precursor materials, the perovskite crystals contain dissolved oxygen.[30] The concentration ratio of this dissolved oxygen and traps will decide the temporal progress of the PL enhancement. If the trap concentration is much lower than the concentration of oxygen in the crystal, the dissolved oxygen is sufficient to cure all traps. In this scenario the PL increase will be independent of surrounding atmosphere, and it will progress at a steady rate as the reaction zone expands when the charge diffusion length increases due to progressing light curing. This process can be expected to be quite fast. If, on the contrary, the trap concentration is much higher than the concentration of dissolved oxygen, then the oxygen "fuel" has to be replenished through diffusion from the crystal surface toward the interior of the crystal. This is expected to be a quite slow process.[30] Which of the situations prevails is expected to depend on the experimental conditions for sample preparation and can be tested by performing the PL experiments with the perovskite crystals immersed in an inert atmosphere.

We measured and compared the PL enhancement temporal progress for micrometer-sized perovskite crystals in air and argon atmosphere (Figure 4a). When the ambient air atmosphere in contact with the perovskite film is replaced with argon, only the initial fast PL increase, very similar to that observed in air, is present (Phase I), while the slow Phase II accounting for most of the PL increase in air is totally absent in argon (Figure 4a). Thus, when diffusion of oxygen from the crystal/atmosphere interface toward the interior of the crystal is not possible, the slow PL increase is absent. These experimental observations give a strong indication that diffusion of oxygen toward the interior of the crystal is the rate-limiting step of the trap curing photochemical process. We have published a detailed analysis of PL charge dynamics during the PL enhancement and a mechanistic view on the process including discussion of possible diffusion of the reaction products (cured defects) and reactants (defects) elsewhere.[30]

The ratio of Phase I to Phase II PL increase in a perovskite microcrystal in principle contains information about the relative contributions of PL quenching in the surface layer and interior of the crystal. Assuming a homogeneous trap distribution throughout the crystal, a static (charge diffusion length ≪ 100 nm) picture would suggest that Phase I of the PL increase corresponds to quenching in the surface layer defined by the ∼100 nm light penetration depth; Phase-II PL increase would then correspond to bulk quenching fueled by diffusion of oxygen/oxygen-related species from the surface to the interior of the crystal. For the typical crystal dimensions studied here, light penetration depth and charge diffusion lengths, one would expect a ∼1/10 ratio of Phase I/Phase II. In reality, this ratio was observed to be 1/50 to 1/100 (Figure 4a). A dynamic view

DOI: 10.1021/acs.jpclett.5b02033
J. Phys. Chem. Lett. 2015, 6, 4171−4177

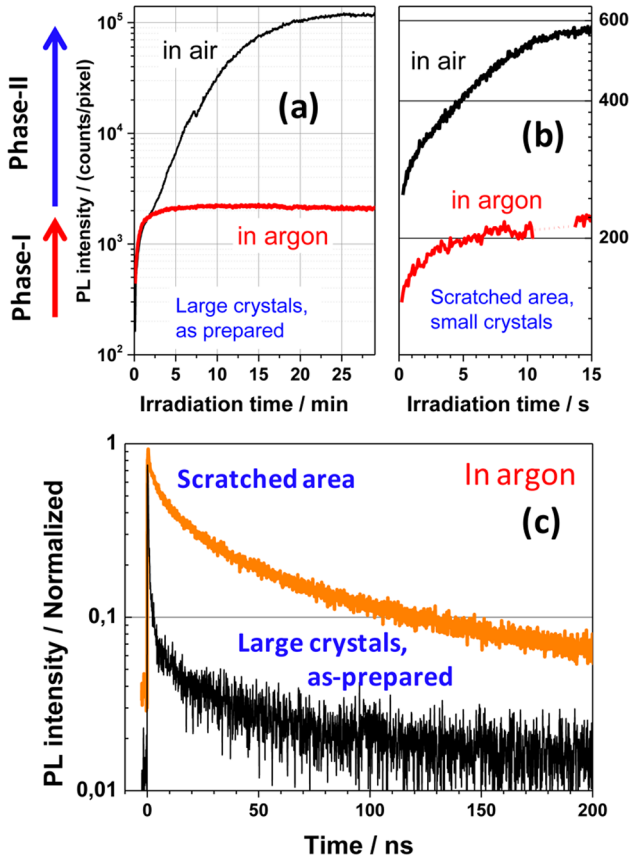

Figure 4. PL enhancement of large (a) and small (b) perovskite crystals in ambient air and in argon (λ_{ex} = 514 nm, 1 W/cm^2). Phase I: enhancement due to the consumption of the oxygen dissolved in the material (identical in air and in argon). Phase II: further PL enhancement that requires oxygen diffusion from the surface to the bulk (does not occur in argon). (c) Normalized PL kinetics measured in the as-prepared micrometer-sized crystals and scratched area (<100 nm grains) of the sample in argon (λ_{ex} = 640 nm, repetition rate 2.5 MHz, 0.1 W/cm^2, IRF width ≈ 100 ps). The sample was kept in argon for 5 min before starting the experiment. The total light exposure of the as-prepared sample during the kinetic acquisition was equal to the irradiation dose that corresponds to ∼1 min irradiation under the conditions of the experiment shown in the panel a.

on the quenching process helps to understand this. As the quenching traps are deactivated in the surface layer and charge diffusion length concomitantly becomes longer they will diffuse out of the cured surface layer and get quenched deeper down in the crystal, where there still is a higher concentration of traps. This process is part of the reaction zone progress previously discussed and will suppress the PL intensity at early times (Phase I) until larger volumes of the crystal have been "cleaned" from traps. The PL decay kinetics on the nanosecond time scale is a good marker of this process.[30] At the earliest times after onset of illumination the decay is very short (few nanoseconds); at intermediate times (∼1 min) it is highly multiexponential with both very short and very long (several hundred of nanoseconds) lifetimes, reflecting highly quenched and nonquenched PL, respectively.[30]

We also studied the atmosphere dependence of the PL enhancement of small (∼100 nm) crystals produced by scratching of the perovskite film. Both in argon (Figure 4b (red curve)) and in air (Figure4b (black curve) and 2 (red curve)) the PL increase caused by illumination exhibits an immediate (within the 100 ms resolution of the experiment) rise of the PL intensity (Figure 4b); however, only in air was a substantial further rise an the time scale of seconds observed (Figure 4b). Thus, qualitatively the behavior of small and larger crystals is similar; the difference is on the time scale. The PL lifetime of a scratched area (small particles) kept in Ar is much longer than that from an as-prepared large micrometer-sized "un-cured" crystal in Ar (Figure 4c), and very similar to that of intentionally photocured large perovskite crystals.[30] This finding can be understood as a result of the fast and efficient trap passivation of the small crystals, with the dissolved bulk oxygen as the reactant.

To understand the behavior of the small perovskite crystals it is necessary to consider the statistical properties of trap distribution in the nanocrystals and its consequences for PL properties. Mathematically this problem is very close to that of quenching of mobile excitons in spatial domains that was extensively studied theoretically in the 1970s in application to the phenomenon of exciton−exciton annihilation observed in photosynthetic molecular aggregates and polymers.[34−36] When decreasing the size of crystals, at some point, depending on the trap concentration, each nanocrystal may contain no or only very few traps, as a result of the Poissonian statistics of trap distribution. At this point PL of a crystal has a "digital" behavior—no traps leads to high PL already at the earliest times (no curing needed) and one or more traps cause perfect quenching (because the charge diffusion length is limited by trapping; without traps, charges probe the whole volume of the small crystal). The trap deactivation through the photochemical process leads to the PL blinking phenomena reported elsewhere.[9] Analysis of the on/off blinking of individual nanocrystals[9] and other literature data[18] gives an estimate of the trap densities of 10^{15} to 10^{16} cm^{-3}, therefore, it can be concluded that the smallest crystals studied in our experiments here (∼100 nm)^3 = 10^6 nm^3 = 10^{-15} cm^3 may contain no or just very few PL quenching traps. This implies that there is a significant fraction (few tens of percent) of small crystals having no traps, which exhibit instantaneous high PL. Crystals with only one, or a few, quenchers are easily and rapidly photocured with the help of the bulk dissolved oxygen. These two effects together lead to the observed rapid increase in PL intensity of small 100 nm sized perovskite crystals.

What is the nature of these bulk traps that can be deactivated by light? This we cannot tell with certainty, but the candidates are numerous, as discussed in literature. Theoretical calculations predict that the most likely defects in methylammonium (MA) lead iodide are lead vacancies, interstitial iodide, and MA-lead antisite substitutions for iodide-rich/lead-poor growth conditions and interstitial MA and iodide vacancies for the opposite, iodide-poor/lead-rich growth conditions.[15−17] Several studies have proposed defects on the surface of the materials,[5,37] but, as previously discussed, in our samples the defects must also be located in the bulk. Indeed, the existence of bulk defects in OMH perovskites has been suggested in some experimental and theoretical studies.[24,25] In our case, the concentration of I$^-$ ions and lead-iodide complex anions in the PbI_2+MAI precursor is usually higher than in other precursors (e.g., $PbCl_2$+MAI; $Pb(Ac)_2$+MAI).[16,38] Therefore, deep bulk trap sites are likely to occur in our perovskite crystals, resulting from the employed equimolar deposition route.[16−18] Alternatively, metallic lead clusters could act as nonradiative recombination sites. These have recently been experimentally verified to exist throughout the bulk of the crystals by XPS

DOI: 10.1021/acs.jpclett.5b02033
J. Phys. Chem. Lett. 2015, 6, 4171−4177

spectroscopy.[39] Obviously, more studies are needed to identify the nature of the photoconvertible defects responsible for the PL enhancement effect.

Now let us examine the PL of micrometer-sized crystals with high spatial resolution. The PL enhancement characteristic time and the enhancement factor strongly varied within one crystal (Figure 5 and in Movie 2). Such inhomogeneity indicates that

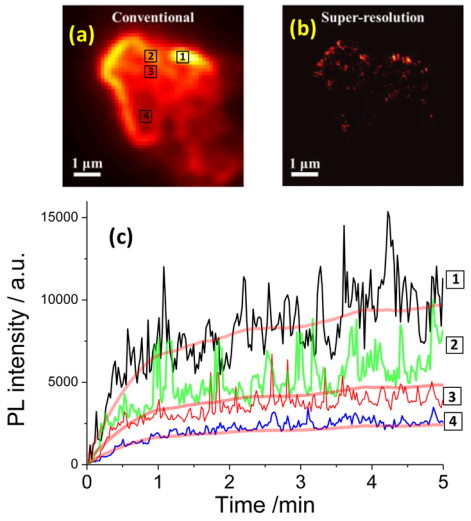

Figure 5. Differential super-resolution optical imaging. (a) The accumulated image (sum of all 500 frames with exposure time of 0.1 s per frame taken every 1.32 s) of a large perovskite crystal under continuous excitation of 0.2 W/cm^2. The whole movie can be found in the SI (Movie 2). (b) Super-resolution image shows localized clusters less than 100 nm in size responsible for light emission (emitting sites). (c) PL intensity (counts per pixel) transient measured locally from the squares marked in panel a; the noise level of the experiment is much smaller than the observed signal fluctuations. The thick red lines are scaled PL intensity of the whole crystal; this data was additionally smoothed.

the observed several-micrometer-sized grains are actually polycrystals. After a certain period of PL enhancement, with rates quite similar for different spatial locations, the PL of some local sites started to exhibit blinking.[9,14,19] Figure 5c shows PL transients of several small areas (0.5 μm × 0.5 μm) of a piece of the perovskite material. Actually, the blinking sites showed a much higher PL brightness per unit area in comparison with the surrounding areas with stable PL. One can see the process more clearly in the movie (Movie 2 in SI), where the PL of the object starts from just several blinking diffraction-limited spots, and as the time progresses, the number of such bright spots increases and the area between the spots starts to emit, too. It was the PL blinking of the sample that allowed us to apply an optical super-resolution method based on emission localization (a STORM-like method[40,41]) and obtain a PL image of the perovskite crystal with spatial resolution below 10 nm.

Using a differential super-resolution localization imaging technique[40,41] (see SI for description) we were able to determine the spatial location of this bright PL with accuracy better than 10 nm. Each dot on the image in Figure S1e gives the location of the emission measured for one particular frame of the movie. As one can see, the dots form closely packed clusters <100 nm in size, indicating that the PL predominantly stems from very localized emitting sites (or emitting volumes) <100 nm in size (Figure 5b).

We propose two alternative hypotheses to the origin of the emitting sites: a small defect-free crystallite or a local area with high radiative recombination rate. Imagine a small (<100 nm) crystallite located on top of a much larger crystal or agglomerate. Charge carries become locally confined in these smaller crystallites and therefore are unaffected by the deep trapping sites present in the bulk of the large crystal. Upon light irradiation, the concentration of defects is reduced and at a certain moment just one defect per "island" is left. Because the diffusion length of charge carriers without defects is larger than the size of the "island",[33] then just one defect is enough to quench completely the "island's" PL. As soon as this defect is cured, the "island" starts to emit with high PL quantum yield. When the defect is reactivated again to its active state, PL of the "island" is switched "off". In this way, the "island" is driven between "on" and "off" states, which is experimentally observed as PL blinking. We suggest that the charge traps leading to PL blinking of individual perovskite crystals previously reported by Tian et al.[9] are the same defects we discuss in the current contribution in relation to the PL light-induced enhancement effect. A connection between PL blinking and PL enhancement phenomenon was recently also suggested for individual $MAPbBr_3$ nanoparticles.[11]

The second idea is that spatially localized PL comes from spatially localized excited states—a concept analogous to energy funneling often observed in organic semiconductors and molecular aggregates.[42,43] Pure band-to-band emission can happen at any place of the crystal. To create an emitting site one needs to bind (at least temporary) the charge carries to a localized defect. It does not contradict the whole previous discussion about PL quenching traps because, depending on the nature, defect states in semiconductors can also lead to effective radiative decay. Such phenomena occur, for example, in phosphors where so-called color centers give red-shifted luminescence.[26] Here we speculate that such emissive defect-associated states can be very shallow but still increase the probability of electron−hole recombination at a particular spatial location. It is well known that localization of the excited states in crystal solids can be induced by local dynamic or static disorder−so-called Anderson localization. Localization of electron and hole wave functions with a radius of several nanometers due to the disorder created in the perovskites crystal by randomly rotating methylammonium molecules has been recently theoretically predicted.[44] Obviously more studies are needed to prove this hypothesis, and we are currently working on correlating super-resolution images and images obtained by electron microscopy to see the morphology of the emitting regions. PL spectroscopy and microscopy at low temperature in combination with SEM of the same sample will help to shed light on this fundamental issue.

In conclusion, we observed that light-induced photoluminescence (PL) enhancement in the OMH perovskite $CH_3NH_3PbI_3$ strongly depends on the size of the crystals. For small (~100 nm or less) crystallites PL enhancement occurs on the subsecond time scale, whereas for crystals of tens of micrometers size it typically takes an hour at one sun excitation power density in air to reach saturation of the PL intensity. The origin of PL enhancement is a photochemical reaction involving oxygen,[14,30] that passivates deep-lying trapping defects. We found that these defects must be located both at the surface and in the bulk of the crystals. The characteristic enhancement time is limited by an interplay between the crystal thickness, the excitation light penetration depth, and the rate of quencher

DOI: 10.1021/acs.jpclett.5b02033
J. Phys. Chem. Lett. 2015, 6, 4171−4177

deactivation. A super-resolution optical imaging technique identified emitting sites in perovskite films—localized emitting areas of <100 nm in diameter. Our hypothesis is that an emitting site can be either a small crystallite free from PL quenching defects or a spatially localized state in a large crystal with increased radiative recombination probability.

■ ASSOCIATED CONTENT

Supporting Information

The Supporting Information is available free of charge on the ACS Publications website at DOI: 10.1021/acs.jpclett.5b02033.

Experimental section; Differential super-resolution localization imaging. (PDF)

Movie 1: PL enhancement by mechanical scratching of the sample. (AVI)

Movie 2: Different PL enhancement behavior within one crystal. (AVI)

■ AUTHOR INFORMATION

Corresponding Author

*E-mail: Ivan.Scheblykin@chemphys.lu.se.

Notes

The authors declare no competing financial interest.

■ ACKNOWLEDGMENTS

This study was financially supported by the Swedish Research Council, the Knut & Alice Wallenberg Foundation, the Crafoord Foundation, the Carl Trygger Foundation, the Swedish Energy Agency, and the Marcus and Amalia Wallenberg Memorial Fund.

■ REFERENCES

(1) Green, M. A.; Ho-Baillie, A.; Snaith, H. J. The Emergence of Perovskite Solar Cells. *Nat. Photonics* **2014**, *8*, 506−514.

(2) Stranks, S. D.; Snaith, H. J. Metal-Halide Perovskites for Photovoltaic and Light-Emitting Devices. *Nat. Nanotechnol.* **2015**, *10*, 391−402.

(3) Tan, Z.-K.; Moghaddam, R. S.; Lai, M. L.; Docampo, P.; Higler, R.; Deschler, F.; Price, M.; Sadhanala, A.; Pazos, L. M.; Credgington, D.; et al. Bright Light-Emitting Diodes Based on Organometal Halide Perovskite. *Nat. Nanotechnol.* **2014**, *8*, 687−692.

(4) Deschler, F.; Price, M.; Pathak, S.; Klintberg, L. E.; Jarausch, D.-D.; Higler, R.; Hüttner, S.; Leijtens, T.; Stranks, S. D.; Snaith, H. J.; et al. High Photoluminescence Efficiency and Optically Pumped Lasing in Solution-Processed Mixed Halide Perovskite Semiconductors. *J. Phys. Chem. Lett.* **2014**, *5*, 1421−1426.

(5) Xing, G.; Mathews, N.; Lim, S. S.; Yantara, N.; Liu, X.; Sabba, D.; Grätzel, M.; Mhaisalkar, S.; Sum, T. C. Low-Temperature Solution-Processed Wavelength-Tunable Perovskites for Lasing. *Nat. Mater.* **2014**, *13*, 476−480.

(6) Im, J.-H.; Lee, C.-R.; Lee, J.-W.; Park, S.-W.; Park, N.-G. 6.5% Efficient Perovskite Quantum-Dot-Sensitized Solar Cell. *Nanoscale* **2011**, *3*, 4088−4093.

(7) Zhang, F.; Zhong, H.; Chen, C.; Wu, X.; Hu, X.; Huang, H.; Han, J.; Zou, B.; Dong, Y. Brightly Luminescent and Color-Tunable Colloidal $CH_3NH_3PbX_3$ (X = Br, I, Cl) Quantum Dots: Potential Alternatives for Display Technology. *ACS Nano* **2015**, *9*, 4533−4542.

(8) Gonzalez-Carrero, S.; Galian, R. E.; Perez-Prieto, J. Maximizing the Emissive Properties of $CH_3NH_3PbBr_3$ Perovskite Nanoparticles . *J. Mater. Chem. A* **2015**, *3*, 9187−9193.

(9) Tian, Y.; Merdasa, A.; Peter, M.; Abdellah, M.; Zheng, K.; Ponseca, C. S.; Pullerits, T.; Yartsev, A.; Sundstrom, V.; Scheblykin, I. G. Giant Photoluminescence Blinking of Perovskite Nanocrystals Reveals Single-Trap Control of Luminescence. *Nano Lett.* **2015**, *15*, 1603−1608.

(10) Zhu, F.; Men, L.; Guo, Y.; Zhu, Q.; Bhattacharjee, U.; Goodwin, P. M.; Petrich, J. W.; Smith, E. A.; Vela, J. Shape Evolution and Single Particle Luminescence of Organometal Halide Perovskite Nanocrystals. *ACS Nano* **2015**, *9*, 2948−2959.

(11) Tachikawa, T.; Karimata, I.; Kobori, Y. Surface Charge Trapping in Organolead Halide Perovskites Explored by Single-Particle Photoluminescence Imaging. *J. Phys. Chem. Lett.* **2015**, *6*, 3195−3201.

(12) Sum, T. C. T.; Mathews, N. Advancements in Perovskite Solar Cells: Photophysics behind the Photovoltaics. *Energy Environ. Sci.* **2014**, *7*, 2518−2534.

(13) Noel, N. K.; Abate, A.; Stranks, S. D.; Parrott, E.; Burlakov, V.; Goriely, A.; Snaith, H. J. Enhanced Photoluminescence and Solar Cell Performance via Lewis Base Passivation of Organic-Inorganic Lead Halide Perovskites. *ACS Nano* **2014**, *8*, 9815−9821.

(14) Galisteo-Lopez, J. F.; Anaya, M.; Calvo, M. E.; Miguez, H. Environmental Effects on the Photophysics of Organic-Inorganic Halide Perovskites. *J. Phys. Chem. Lett.* **2015**, *6*, 2200−2205.

(15) Yin, W.-J.; Shi, T.; Yan, Y. Unusual Defect Physics in $CH_3NH_3PbI_3$ Perovskite Solar Cell Absorber. *Appl. Phys. Lett.* **2014**, *104*, 063903.

(16) Buin, A.; Pietsch, P.; Xu, J.; Voznyy, O.; Ip, A. H.; Comin, R.; Sargent, E. H. Materials Processing Routes to Trap-Free Halide Perovskites. *Nano Lett.* **2014**, *14*, 6281−6286.

(17) Williams, S. T.; Chueh, C.-C.; Jen, A. K.-Y. Navigating Organo-Lead Halide Perovskite Phase Space via Nucleation Kinetics toward a Deeper Understanding of Perovskite Phase Transformations and Structure-Property Relationships. *Small* **2015**, *11*, 3088−3096.

(18) Stranks, S. D.; Nayak, P. K.; Zhang, W.; Stergiopoulos, T.; Snaith, H. J. Formation of Thin Films of Organic-Inorganic Perovskites for High-Efficiency Solar Cells. *Angew. Chem., Int. Ed.* **2015**, *54*, 3240−3248.

(19) Stranks, S. D.; Burlakov, V. M.; Leijtens, T.; Ball, J. M.; Goriely, A.; Snaith, H. J. Recombination Kinetics in Organic-Inorganic Perovskites: Excitons, Free Charge, and Subgap States. *Phys. Rev. Appl.* **2014**, *2*, 1−8.

(20) D'Innocenzo, V.; Srimath Kandada, A. R.; De Bastiani, M.; Gandini, M.; Petrozza, A. Tuning the Light Emission Properties by Band Gap Engineering in Hybrid Lead Halide Perovskite. *J. Am. Chem. Soc.* **2014**, *136*, 17730−17733.

(21) DeQuilettes, D. W.; Vorpahl, S. M. S.; Stranks, S. D. S.; Nagaoka, H.; Eperon, G. E.; Ziffer, M. E.; Snaith, H. J.; Ginger, D. S. Impact of Microstructure on Local Carrier Lifetime in Perovskite Solar Cells. *Science* **2015**, *348*, 683−686.

(22) Guo, Z.; Manser, J. S.; Wan, Y.; Kamat, P. V.; Huang, L. Spatial and Temporal Imaging of Long-Range Charge Transport in Perovskite Thin Films by Ultrafast Microscopy. *Nat. Commun.* **2015**, *6*, 7471.

(23) Vrućinić, M.; Matthiesen, C.; Sadhanala, A.; Divitini, G.; Cacovich, S.; Dutton, S. E.; Ducati, C.; Atatüre, M.; Snaith, H.; Friend, R. H.; et al. Local Versus Long-Range Diffusion Effects of Photoexcited States on Radiative Recombination in Organic-Inorganic Lead Halide Perovskites. *Adv. Sci.* **2015**, *2*, n/a.

(24) Bischak, C. G.; Sanehira, E. M.; Precht, J. T.; Luther, J. M.; Ginsberg, N. S. Heterogeneous Charge Carrier Dynamics in Organic-Inorganic Hybrid Materials: Nanoscale Lateral and Depth-Dependent Variation of Recombination Rates in Methylammonium Lead Halide Perovskite Thin Films. *Nano Lett.* **2015**, *15*, 4799−4807.

(25) Kim, J.; Lee, S.-H.; Lee, J. H.; Hong, K.-H. The Role of Intrinsic Defects in Methylammonium Lead Iodide Perovskite. *J. Phys. Chem. Lett.* **2014**, *5*, 1312−1317.

(26) Pelant, I.; Valenta, J. *Luminescence Spectroscopy of Semiconductors*; Oxford University Press: Oxford, U.K., 2012.

(27) Christians, J. A.; Manser, J. S.; Kamat, P. V. The Multifaceted Excited State of $CH_3NH_3PbI_3$. Charge Separation, Recombination, and Trapping. *J. Phys. Chem. Lett.* **2015**, *6*, 2086−2095.

(28) Hoke, E. T.; Slotcavage, D. J.; Dohner, E. R.; Bowring, A. R.; Karunadasa, H. I.; McGehee, M. D. Reversible Photo-Induced Trap Formation in Mixed-Halide Hybrid Perovskites for Photovoltaics. *Chem. Sci.* **2015**, *6*, 613−617.

DOI: 10.1021/acs.jpclett.5b02033
J. Phys. Chem. Lett. 2015, 6, 4171−4177

(29) Samiee, M.; Konduri, S.; Ganapathy, B.; Kottokkaran, R.; Abbas, H. A.; Kitahara, A.; Joshi, P.; Zhang, L.; Noack, M.; Dalal, V. Defect Density and Dielectric Constant in Perovskite Solar Cells. *Appl. Phys. Lett.* **2014**, *105*, 153502.
(30) Tian, Y.; Peter, M.; Unger, E.; Abdellah, M.; Zheng, K.; Pullerits, T.; Yartsev, A.; Sundström, V.; Scheblykin, I. G. Mechanistic Insights into Perovskite Photoluminescence Enhancement: Light Curing with Oxygen Can Boost Yield Thousandfold. *Phys. Chem. Chem. Phys.* **2015**, *17*, 24978.
(31) Sun, S.; Salim, T.; Mathews, N.; Duchamp, M.; Boothroyd, C.; Xing, G.; Sum, T. C.; Lam, Y. M. The Origin of High Efficiency in Low-Temperature Solution-Processable Bilayer Organometal Halide Hybrid Solar Cells. *Energy Environ. Sci.* **2014**, *7*, 399.
(32) Xing, G.; Mathews, N.; Sun, S.; Lim, S. S.; Lam, Y. M.; Grätzel, M.; Mhaisalkar, S.; Sum, T. C. Long-Range Balanced Electron- and Hole-Transport Lengths in Organic-Inorganic $CH_3NH_3PbI_3$. *Science* **2013**, *342*, 344−347.
(33) Stranks, S. D.; Eperon, G. E.; Grancini, G.; Menelaou, C.; Alcocer, M. J. P.; Leijtens, T.; Herz, L. M.; Petrozza, A.; Snaith, H. J. Electron-Hole Diffusion Lengths Exceeding 1 Micrometer in an Organometal Trihalide Perovskite Absorber. *Science* **2013**, *342*, 341−344.
(34) Paillotin, G.; Geacintov, N.; Breton, J. A Master Equation Theory of Fluorescence Induction, Photochemical Yield, and Singlet-Triplet Exciton Quenching in Photosynthetic Systems. *Biophys. J.* **1983**, *44*, 65−77.
(35) Scheblykin, I.; Varnavsky, O.; Bataiev, M.; Sliusarenko, O.; Van Der Auweraer, M.; Vitukhnovsky, A. Non-Coherent Exciton Migration in J-Aggregates of the Dye THIATS: Exciton-Exciton Annihilation and Fluorescence Depolarization. *Chem. Phys. Lett.* **1998**, *298*, 341−350.
(36) Sahoo, D.; Tian, Y.; Sforazzini, G.; Anderson, H. L.; Scheblykin, I. G. Photo-Induced Fluorescence Quenching in Conjugated Polymers Dispersed in Solid Matrices at Low Concentration. *J. Mater. Chem. C* **2014**, *2*, 6601−6608.
(37) Nie, W.; Tsai, H.; Asadpour, R.; Blancon, J.-C.; Neukirch, A. J.; Gupta, G.; Crochet, J. J.; Chhowalla, M.; Tretiak, S.; Alam, M. A.; et al. High-Efficiency Solution-Processed Perovskite Solar Cells with Millimeter-Scale Grains. *Science* **2015**, *347*, 522−525.
(38) Zhang, H.; Jang, J.; Liu, W.; Talapin, D. V. Colloidal Nanocrystals with Inorganic Halide, Pseudohalide, and Halometallate Ligands. *ACS Nano* **2014**, *8*, 7359−7369.
(39) Sadoughi, G.; Starr, D. E.; Handick, E.; Stranks, S. D.; Gorgoi, M.; Wilks, R. G.; Baer, M.; Snaith, H. J. Observation and Mediation of the Presence of Metallic Lead in Organic-Inorganic Perovskite Films. *ACS Appl. Mater. Interfaces* **2015**, *7*, 13440−13444.
(40) Rust, M. J.; Bates, M.; Zhuang, X. Sub-Diffraction-Limit Imaging by Stochastic Optical Reconstruction Microscopy (STORM). *Nat. Methods* **2006**, *3*, 793−795.
(41) Ristanović, Z.; Hofmann, J. P.; De Cremer, G.; Kubarev, A. V.; Rohnke, M.; Meirer, F.; Hofkens, J.; Roeffaers, M. B. J.; Weckhuysen, B. M. Quantitative 3D Fluorescence Imaging of Single Catalytic Turnovers Reveals Spatiotemporal Gradients in Reactivity of Zeolite H-ZSM-5 Crystals upon Steaming. *J. Am. Chem. Soc.* **2015**, *137*, 6559−6568.
(42) Yu, J.; Hu, D.; Barbara, P. F. Unmasking Electronic Energy Transfer of Conjugated Polymers by Suppression of O_2 Quenching. *Science* **2000**, *289*, 1327−1330.
(43) Merdasa, A.; Jiménez, A. J.; Camacho, R.; Meyer, M.; Würthner, F.; Scheblykin, I. G.; Jiménez, Á.; Wu, F. Single Lévy States-Disorder Induced Energy Funnels in Molecular Aggregates. *Nano Lett.* **2014**, *14*, 6774−6781.
(44) Ma, J.; Wang, L.-W. Nanoscale Charge Localization Induced by Random Orientations of Organic Molecules in Hybrid Perovskite $CH_3NH_3PbI_3$. *Nano Lett.* **2015**, *15*, 248−253.

DOI: 10.1021/acs.jpclett.5b02033
J. Phys. Chem. Lett. 2015, 6, 4171−4177